STP 1599, 2017 / available online at www.astm.org / doi: 10.1520/STP159920160106

Samuel V. Glass,[1] Stanley D. Gatland II,[2] Kohta Ueno,[3]
and Christopher J. Schumacher[4]

Analysis of Improved Criteria for Mold Growth in ASHRAE Standard 160 by Comparison with Field Observations

Citation

Glass, S. V., Gatland II, S. D., Ueno, K., and Schumacher, C. J., "Analysis of Improved Criteria for Mold Growth in ASHRAE Standard 160 by Comparison with Field Observations," *Advances in Hygrothermal Performance of Building Envelopes: Materials, Systems and Simulations, ASTM STP1599*, P. Mukhopadhyaya and D. Fisler, Eds., ASTM International, West Conshohocken, PA, 2017, pp. 1–27, http://dx.doi.org/10.1520/STP159920160106[5]

ABSTRACT

ASHRAE Standard 160, *Criteria for Moisture-Control Design Analysis in Buildings*, was published in 2009. The standard sets criteria for moisture design loads, hygrothermal analysis methods, and satisfactory moisture performance of the building envelope. One of the evaluation criteria specifies conditions necessary to avoid mold growth. The current standard requires that the 30-day running average relative humidity at the material surface be less than 80 % when the 30-day running average surface temperature is between 5°C (41°F) and 40°C (104°F). This criterion was intended to strike a balance between the need for simplicity to make the standard useful and the complex reality of mold growth, which varies with mold species and depends on the type of material, water activity, temperature, and other factors. Since the standard was

Manuscript received July 15, 2016; accepted for publication November 1, 2016.

[1]USDA Forest Service Forest Products Laboratory, Building and Fire Sciences, 1 Gifford Pinchot Dr., Madison, WI 53726

[2]CertainTeed Corp., Malvern Innovation Center, 18 Moores Rd., Malvern, PA 19355

[3]Building Science Corp., 70 Main St., Westford, MA 01886

[4]RDH Building Science Laboratories, 167 Lexington Ct., Unit 6, Waterloo, ON, N2J 4R9, Canada

[5]ASTM Symposium on *Advances in Hygrothermal Performance of Building Envelopes: Materials, Systems and Simulations* on October 26–27, 2016 in Orlando, FL.

published, many practitioners have maintained that the mold criterion is too stringent. Assemblies known to have satisfactory performance in the field do not meet the criterion under hygrothermal simulation. A recent addendum to ASHRAE Standard 160 replaced the simplified mold criterion with a state-of-the-art empirical model that describes mold growth and decline over time using a mold index. This model takes into account the sensitivity of the material, the surface temperature, and the surface relative humidity. This paper provides an overview of the mold index model and a series of comparisons between field observations of visible mold growth or lack thereof on wood-based sheathing and model predictions that use measured surface temperature and relative humidity values as inputs. The field data are from published studies on above-grade wood-frame wall assemblies and roof assemblies covering a range of climate zones. Our analysis indicates that the current 30-day criterion in ASHRAE Standard 160 fails many assemblies in which visible mold growth did not occur. In contrast, the mold index model predictions give better agreement with observations.

Keywords

moisture control, building envelope, hygrothermal performance, hygrothermal analysis, simulation, mold growth, mold index, durability, failure criteria, ASHRAE Standard 160

Introduction

ASHRAE Standard 160-2009, *Criteria for Moisture-Control Design Analysis in Buildings* [1], provides a standardized set of criteria on how to conduct, evaluate, and report the results of hygrothermal analysis on new and existing building envelope systems. The purpose of the standard is “to specify performance-based design criteria for predicting, mitigating, or reducing moisture damage to the building envelope, materials, components, systems, and furnishings, depending on climate, construction type, and HVAC system operation.” The criteria apply to input parameters including moisture design loads, analytical procedures, and evaluation and use of outputs. Section 4 of the standard, “Criteria for Design Parameters,” addresses how to select design values for initial moisture conditions of building materials, indoor temperatures, indoor relative humidity (RH), building air pressure differentials, air speed and flow, weather data, and rain loads. Section 5, “Criteria for Selecting Analytical Procedures,” sets minimum acceptable requirements for analytical tools capable of performing transient heat and moisture transfer calculations on building envelope assemblies. Section 6, “Moisture Performance Evaluation Criteria,” sets boundaries on conditions necessary to avoid mold growth and corrosion. Comprehensive summary reviews of ASHRAE Standard 160 were provided by TenWolde [2] and Gatland [3] shortly after publication in 2009.

The original mold growth criteria in Section 6.1, “Conditions Necessary to Minimize Mold Growth,” were adopted from three criteria recommended in the

International Energy Agency Report Annex XIV [4]. The section requires meeting the following three conditions to minimize problems associated with mold growth:

a. Thirty-day running average surface RH is less than 80 % when the 30-day running average surface temperature is between 5°C (41°F) and 40°C (104°F)
b. Seven-day running average surface RH is less than 98 % when the seven-day running average surface temperature is between 5°C (41°F) and 40°C (104°F)
c. Twenty-four-hour running average surface RH is less than 100 % when the 24-hour running average surface temperature is between 5°C (41°F) and 40°C (104°F)

These criteria were simplified through "Addendum a" [5] to include only the 30-day running average surface conditions as described earlier.

Since the standard was published, many users have considered the mold growth evaluation criteria to be too stringent. A number of researchers and practitioners have reported that assemblies known to fail the criteria in hygrothermal simulation have satisfactory performance in the field [6–10]. Scientific literature also indicates that mold growth requires a much more complex description than the simple 30-day criterion [11–19].

Recently, "Addendum e" was proposed to improve the mold evaluation criteria in ASHRAE Standard 160 [20]. The proposed changes are based on the updated mold growth model developed by Ojanen and colleagues [21].

The objective of this paper is to compare the predictive ability of the simple 30-day criterion to the mold growth model. The two methods used measured surface RH and temperature as inputs, and results were compared with field observations of mold growth (or lack thereof) in various building envelope assemblies. The development and key features of the mold growth model are described in the next section, which is followed by a description of analysis methods, results and discussion, and conclusions.

Overview of Viitanen's Mold Growth Model

The mathematical mold growth model developed by Viitanen and colleagues is based on empirical data and has been updated through multiple improvements over time [11–13, 21–26]. Original measurements were based on pine and spruce sapwood, but the number of materials tested has grown over time as will be discussed here.

The most recent version of the model correlates a mold index scale between zero and six with increasing descriptions of mold growth rates based on experimental measurements. Table 1 describes the amount of growth based on visual observations using both a microscope and the naked human eye. It is important to note that the mold index value of three corresponds with visual finding of mold growth and production of new spores.

The latest version of the model incorporates four material sensitivity classes that were created to coincide with common building materials used in construction. The materials tested are described in Table 2 along with generalized material groups.

TABLE 1 Description of mold index scale [21,25,26].

Index	Description of Growth Rate	Microscopic Observation	Visual Observation
0	No growth; spores not activated	None	None
1	Initial stages of growth	Small amounts of mold on surface	None
2	—	Several local colonies	None
3	New spores produced	<50 % coverage	<10 % coverage
4	Moderate growth	>50 % coverage	10 %–50 % coverage
5	Plenty of growth	—	>50 % coverage
6	Heavy and tight growth	—	about 100 % coverage

TABLE 2 Mold sensitivity classes for various materials [21].

Sensitivity Class	Materials Used in Experiments	Generalized Material Groups
Very sensitive	Pine sapwood	Untreated wood; includes lots of nutrients for biological growth
Sensitive	Spruce sapwood, glued wooden boards, polyurethane insulation with paper surface	Planed wood, paper-coated products, wood-based boards
Medium resistant	Concrete, aerated and cellular concrete, glass wool, polyester wool	Cement or plastic based materials, mineral fibers
Resistant	Polyurethane insulation with polished surface	Glass and metal products, materials with efficient protective compound treatments

Favorable conditions for mold growth occur when the surface temperature (T) is above 0°C and the surface RH is above a critical value. The critical surface RH value depends on both the material sensitivity class and the surface temperature, as shown in Fig. 1. The mold index increases each hour when favorable conditions exist based on the surface temperature, surface RH, and sensitivity class. The series of equations used in calculating the mold index can be found in Ojanen et al. [21].

Unfavorable conditions exist when the surface temperature is below 0°C or when the surface RH is below the critical value. When conditions are unfavorable, the mold index decreases at a rate that depends on the length of time conditions have been unfavorable and on a decline coefficient that depends on the material. Different materials exhibit different rates of mold index decline; the model accounts for this using a decline coefficient relative to original measurements using pine sapwood, which is given a coefficient of one.

The evolution of the mold index over time is illustrated for a few simple cases under constant temperature and humidity conditions in Fig. 2. The mold index values for different sensitivity classes at 20°C and 95 % RH are depicted in Fig. 2a. Focusing on the sensitive class, the mold index at 20°C and various constant RH levels are shown in Fig. 2b.

FIG. 1 Critical surface RH as a function of surface temperature for different material sensitivity classes, based on the updated Viitanen model [21].

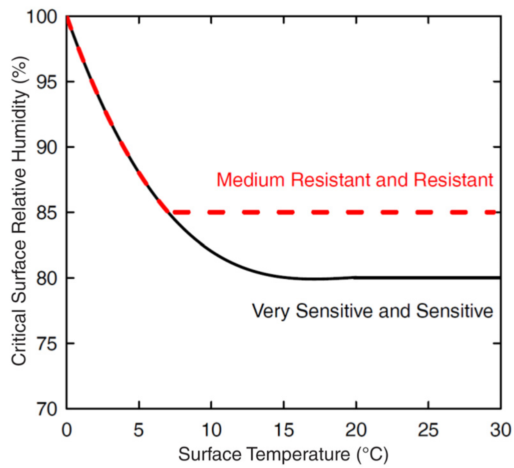

The mold index model has been used as a tool to evaluate the results of a hygrothermal analysis. Recent investigations have compared field measurement results with the results of hygrothermal analysis using the ASHRAE Standard 160-2009 criteria and the most recent Viitanen mold index model [9,10]. Field observations of surface conditions more closely correlate with the Viitanen model. ASHRAE Standard 160-2009 criteria overpredict the risk for mold growth and are not consistent with field observations.

Analysis Methods

The measured data used for the analysis in this paper come from previously published research on moisture performance of above-grade wood-frame wall and roof assemblies. The wall or roof sheathing in these assemblies was oriented strand board (OSB) or plywood. The surface of interest for mold growth was the sheathing surface that faced the insulated cavity. In each study, the assemblies were inspected after a period of monitoring, and researchers recorded visual observations of mold growth or lack thereof on the wood-based sheathing. The analysis in this paper uses the measured surface temperature and RH values as inputs for evaluating mold risk. The following sections describe (1) how surface temperature and RH were either measured or derived from measured parameters; and (2) how analysis was conducted with two different moisture performance evaluation criteria: the first using 30-day running average conditions and the second using the mold index model.

FIG. 2 Predicted mold index versus time under constant conditions based on the updated Viitanen model [21]: (a) 20°C and 95 % RH for each sensitivity class; (b) sensitive class at 20°C for various humidity levels.

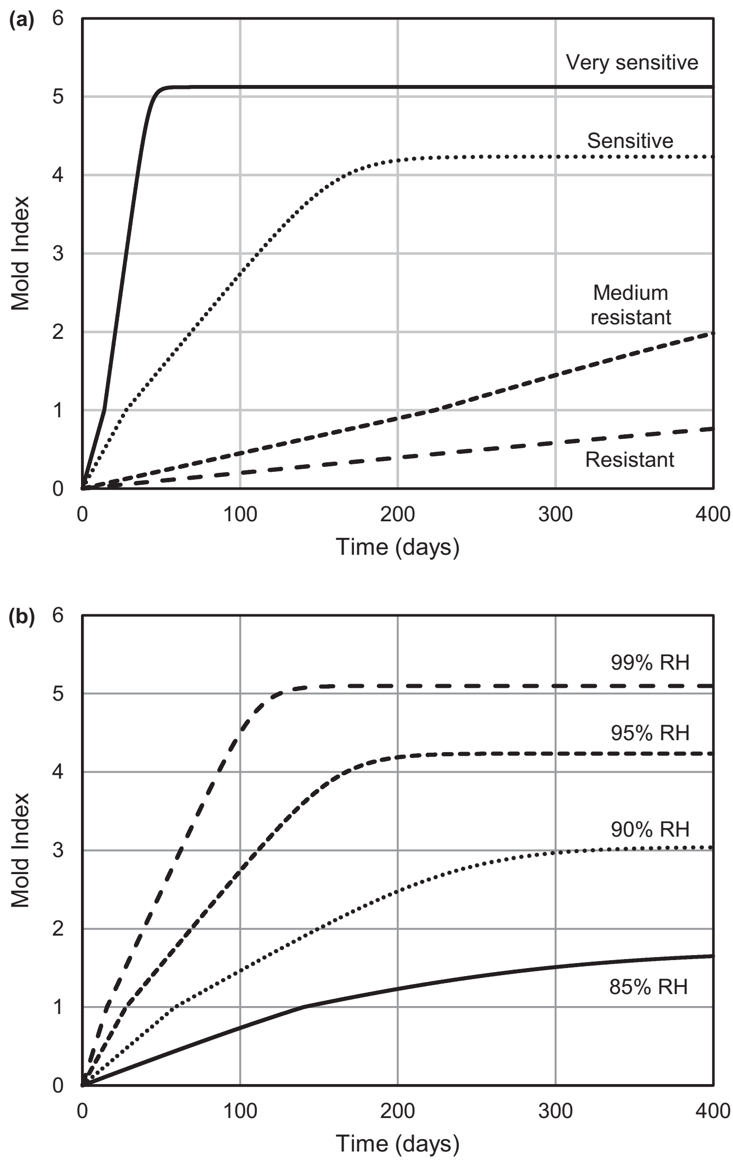

SURFACE TEMPERATURE AND RELATIVE HUMIDITY

Each of the monitored assemblies had an instrumentation package connected to a data acquisition system that recorded values hourly. The assemblies and relevant sensors are depicted in Fig. 3 and Fig. 4. These include wall assemblies with different

FIG. 3 Wall assemblies monitored near Seattle, WA [27]. Interior vapor retarder was 0.1-mm polyethylene (PE), 0.05-mm polyamide (smart vapor retarder, SVR), or none (paint only). The RH/T sensor was placed at the cavity side of the OSB sheathing at the center of the stud cavity, 150 mm below the top plate.

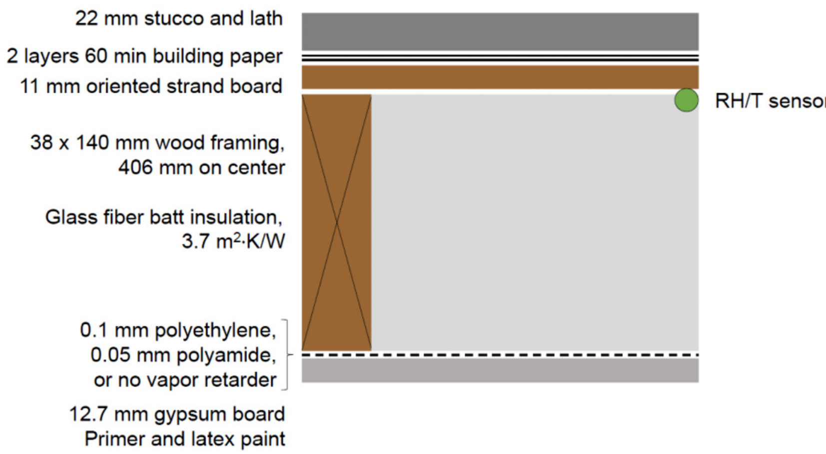

interior vapor retarders in Seattle, WA (Fig. 3) [27], and roof assemblies with different insulation and venting methods in Chicago, IL (Fig. 4 and Table 3) [28]. In the wall and roof assemblies, temperature was measured at the surface of the sheathing. Relative humidity at the sheathing surface was determined three different ways. In the first method, the RH/T sensor was placed directly at the sheathing surface. The RH/T values were then taken directly; no corrections were necessary.

A second method made use of a wood "wafer" sensor equipped with pin electrodes for measurement of wood moisture content (MC) by electrical conductance. This type of sensor, described previously by Carll and TenWolde [29] and Ueno and Straube [30], is a surrogate for humidity and uses the relationship between RH and MC (the sorption isotherm). As noted by Ueno and Lstiburek [28], wafer

FIG. 4 Roof assemblies monitored near Chicago, IL [28]. The RH/T sensor and wafer sensor (not shown) were placed just below the OSB sheathing at the ridge of each assembly.

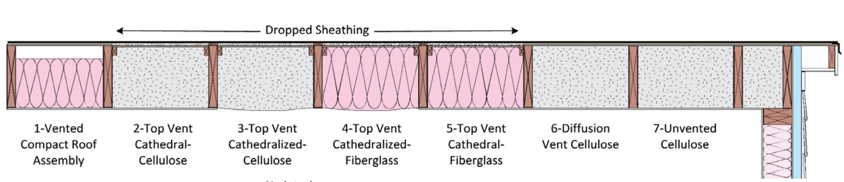

TABLE 3 Description of roof assemblies monitored in Bolingbrook, IL [28].

Designation	Interior	Insulation	Exterior	Ventilation
1 – Vented compact roof	12.7-mm gypsum board, latex paint	Fiberglass batt, 5.3 $m^2 \cdot K/W$	11-mm OSB, #30 felt, asphalt shingle	100-mm air space below sheathing, openings at eave and ridge
2 – Top vent cathedral, cellulose	12.7-mm gypsum board, latex paint	Cellulose, dense packed, 6.7 $m^2 \cdot K/W$	11-mm OSB, mesh, asphalt shingle	Breather mesh ventilation under shingles, eave to ridge
3 – Top vent cathedralized, cellulose	None (open)	Cellulose, dense packed, 6.7 $m^2 \cdot K/W$	11-mm OSB, mesh, asphalt shingle	Breather mesh ventilation under shingles, eave to ridge
4 – Top vent cathedralized, fiberglass	None (open)	Fiberglass batt, 6.7 $m^2 \cdot K/W$	11-mm OSB, mesh, asphalt shingle	Breather mesh ventilation under shingles, eave to ridge
5 – Top vent cathedral, fiberglass	12.7-mm gypsum board, latex paint	Fiberglass batt, 6.7 $m^2 \cdot K/W$	11-mm OSB, mesh, asphalt shingle	Breather mesh ventilation under shingles, eave to ridge
6 – Diffusion vent, cellulose	12.7-mm gypsum board, latex paint	Cellulose, dense packed, 6.7 $m^2 \cdot K/W$	11-mm OSB, #30 felt, asphalt shingle	Ridge "diffusion vent" (glass fiber faced gypsum board)
7 – Unvented, cellulose	12.7-mm gypsum board, latex paint	Cellulose, dense packed, 6.7 $m^2 \cdot K/W$	11-mm OSB, #30 felt, asphalt shingle	Ridge sealed with self-adhered membrane; unvented

sensors can be more reliable than polymeric capacitive RH sensors under high RH conditions over long periods, and they can be useful for understanding seasonal moisture accumulation and drying patterns. The time response of these wood-based sensors is somewhat delayed, which should be understood when interpreting the results. Wood MC was calculated from measured electrical resistance and temperature using equations given by Straube, Onysko, and Schumacher [31]. The RH was then calculated from the wood MC (expressed as a percentage of the dry mass) using Eq 1, which was fit to the generic wood sorption data from the *Wood Handbook* [32] at a temperature of 10°C, which is approximately the annual mean for field conditions. Temperature dependence in the RH/MC relationship is minor and is neglected here.

$$\frac{RH}{100} = 1 - \exp\left[-26.665\left(\frac{MC}{100}\right)^{1.550}\right] \tag{1}$$

In a previous calibration [30], the wafer sensors came to equilibrium with 100 % RH conditions (suspended in air over water in a closed container) at 28 % to 30 % MC, while immersing the wafer sensors in liquid water increased their MC to the 40 % to 45 % range.

A third method involved electrical resistance measurement of sheathing MC. Pin electrodes, electrically insulated except for the tip, were inserted to a depth of 6 mm into the sheathing (nominally the middle). MC and RH were calculated in the same way as described earlier for the wood wafers. Because of the pin location at mid-depth rather than at the surface, this method also had a delayed time response, and RH fluctuations were damped by the moisture storage capacity of the sheathing.

MOISTURE PERFORMANCE EVALUATION CRITERIA

Thirty-Day Criterion

ASHRAE Standard 160-2009 [1] and "Addendum A" [5] specify conditions necessary to minimize mold growth in terms of 30-day running average values of surface RH and temperature. This criterion requires that the 30-day running average RH at the material surface be less than 80 % when the 30-day running average surface temperature is between 5°C and 40°C. This method is illustrated graphically in the "Results and Discussion" section, taking 30-day running average surface temperature and RH values based on hourly values measured at sheathing surfaces in wall and roof assemblies.

Mold Index Model

The updated Viitanen mold index model [21] was evaluated as an alternative to the ASHRAE Standard 160 criteria. Mold index values were calculated at 1-h intervals using this model with measured hourly values of surface temperature and RH at sheathing surfaces in wall and roof assemblies. The following assumptions were made in running the model:

- OSB was modeled using the sensitive class, based on the recommendation of Ojanen et al. [21] for "wood-based boards" (Table 2).
- The initial mold index value at the beginning of the field monitoring studies was assumed to be zero.
- The coefficient for mold index decline on OSB during unfavorable conditions was taken as 0.3 based on the value for spruce, which belongs to the sensitive class.
- The surface quality parameter was interpreted as being zero in all cases in the revised model of Ojanen et al. [21].

Field observations of mold growth or lack thereof did not include microscopy; observations were limited to visual assessment without magnification. The relevant mold index (M) threshold corresponding to visible mold growth is $M = 3$ (Table 1).

Results and Discussion

This section begins with a review of similar prior analyses conducted by the authors. Results of the present analysis are then presented and discussed for each set of building envelope assemblies.

PRIOR ANALYSIS OF WALL AND ROOF ASSEMBLIES

Analysis of experimentally monitored wall and roof assemblies that had no visible mold growth were presented by Glass, Schumacher, and Ueno [9] and summarized by Lstiburek, Ueno, and Musunuru [10]. The assemblies included double-stud walls in Devens, MA (Climate Zone 5A) [33,34]; an unvented cathedral ceiling in Vancouver, BC (Climate Zone 4C) [35]; and a vented attic and unvented cathedralized attic in Coquitlam, BC (Climate Zone 4C) [36]. The results are summarized in Table 4. In all but one case, the 30-day criterion indicated risk of mold growth; that is, the hourly measured surface RH/T conditions led to calculated 30-day running averages that did not stay within the specified "conditions necessary to minimize mold growth." Visible mold growth, however, was not observed in any of the assemblies during disassembly. In all cases, the mold index model, using measured hourly surface RH/T values as inputs, resulted in mold index values less than 3.0, in agreement with observations. The results of this series of comparisons indicate that the mold index model matches reality (i.e., it is not overly conservative), and it avoids "false positives," unlike the 30-day criterion. The comparisons, however, do not provide any information on the predictions of the mold index model for cases in which visible mold growth was observed. This knowledge gap and uncertainty regarding potential "false negatives" was the motivation for the present analysis.

WALL ASSEMBLIES IN SEATTLE

Gatland et al. [27] monitored hygrothermal performance of wood-frame wall assemblies using the Natural Exposure Test Facility located on the campus of Washington State University in Puyallup, WA (Seattle area; Climate Zone 4C). Walls were oriented facing south. The assemblies are depicted in Fig. 3; they differ only in the interior vapor retarder and are denoted as follows:

- Polyethylene (PE)—0.1-mm PE film; literature vapor permeance is 3–5 ng/Pa · s · m^2 [37,38].
- Smart vapor retarder (SVR)—0.05-mm polyamide film; vapor permeance varies from 44 ng/Pa · s · m^2 at a mean RH of 25 % to 280 ng/Pa · s · m^2 at a mean RH of 75 % and exceeds 2000 ng/Pa · s · m^2 at a mean RH of 95 % [38].
- Paint—no vapor retarder other than primer and latex paint on the interior gypsum board; vapor permeance of the coated gypsum board was reported to be as high as 1100 ng/Pa · s · m^2 [39].

TABLE 4 Summary of previous analysis contrasting 30-day criterion with mold index model [9,10].

Assembly Type	Location	Visible Mold Growth?	Performance Model Prediction	
			30-Day Criterion	Mold Index Model
Double-stud walls [33,34]	Devens, MA	No	Mold risk	M < 3
Unvented cathedral ceiling [35]	Vancouver, BC	No	No mold risk	M < 3
Vented attic [36]	Coquitlam, BC	No	Mold risk	M < 3
Unvented cathedralized attic [36]	Coquitlam, BC	No	Mold risk	M < 3

Monitoring began in the summer of 2003. The interior environment was maintained at 21°C and 50 % to 55 % RH. During the spring of 2004, visual examination of the paint wall indicated mold growth on the cavity-side surface of the OSB sheathing.

Hourly surface RH values are plotted in Fig. 5 for each assembly. An expected seasonal trend is observed for all assemblies: RH values peaked during winter and reached a minimum during summer. Wintertime values remained at or near 100 % RH for the paint wall.

Thirty-day running average OSB surface RH values are shown in Fig. 6 for each wall, with the 30-day running average OSB surface temperature in the PE wall. The 30-day running average surface temperature values for the other two walls are not shown because they did not differ appreciably from the values for the PE wall. The 30-day running average surface temperatures remained between 5°C and 40°C during the monitoring period. The 30-day running average surface RH values exceeded 80 % RH in all three cases. Thus, the ASHRAE Standard 160 “Addendum a” criterion for conditions necessary to minimize mold growth was not met for any of the three walls. Visual observations, however, found mold growth on OSB only in the paint wall. For comparison, measured OSB MCs were well in excess of 30 % MC in the paint wall during winter. In contrast, the OSB MCs in the PE and SVR walls peaked at about 16 % and 12 %, respectively, well below values typically associated with risk of mold growth. This analysis confirms that the 30-day criterion is too stringent.

Mold index values calculated from the measured hourly surface RH/T values over the course of the monitoring period are shown in Fig. 7. The mold index for the paint wall increases steadily during winter and reaches a peak value of 3.4 during March, before slowly declining as drying of the OSB surface occurred during warmer conditions. This mold index value above three for the paint wall agrees with the visual observation of mold growth in this wall during the spring of 2004. In contrast, the mold index values for the PE and SVR walls remain below one, in agreement with visual observation of lack of mold growth. In summary, this case illustrates that the mold index model correctly identifies conditions that led to visible mold growth and conditions that did not.

ROOF ASSEMBLIES IN CHICAGO

Ueno and Lstiburek [28] monitored moisture and temperature conditions in a series of residential sloped roof assemblies in a test house located in Bolingbrook, IL (Chicago area; Climate Zone 5A). Roof orientations were east and west. Seven parallel rafter bays were monitored as described in Table 3 and depicted in Fig. 4. All assemblies had OSB roof sheathing and asphalt shingles. Conditions were monitored just below the roof ridge near the OSB sheathing using both an RH/T sensor and a wood wafer sensor. In addition, the MC of the OSB sheathing near the ridge was monitored with moisture pins, with the exception of Roof 6, where the ridge had a diffusion vent rather than OSB. The interior environment was maintained at

FIG. 5 Measured hourly RH values at cavity-side surface of OSB sheathing in Puyallup, WA, for walls with (a) PE, (b) SVR, and (c) no vapor retarder other than paint.

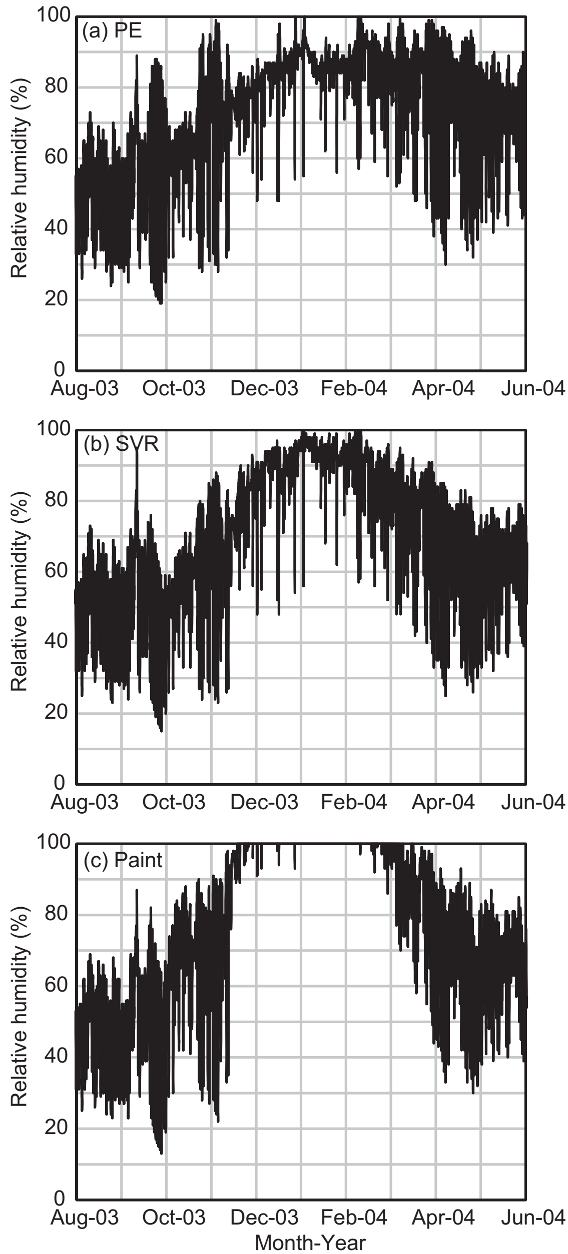

FIG. 6 Thirty-day running average RH values at cavity-side surface of OSB sheathing in Puyallup, WA, for walls with PE, SVR, and paint only. Thirty-day running average OSB surface temperature is shown only for the PE wall; temperatures in other walls were essentially the same. The 80 % RH threshold and the 5°C to 40°C temperature band are indicated with dashed lines.

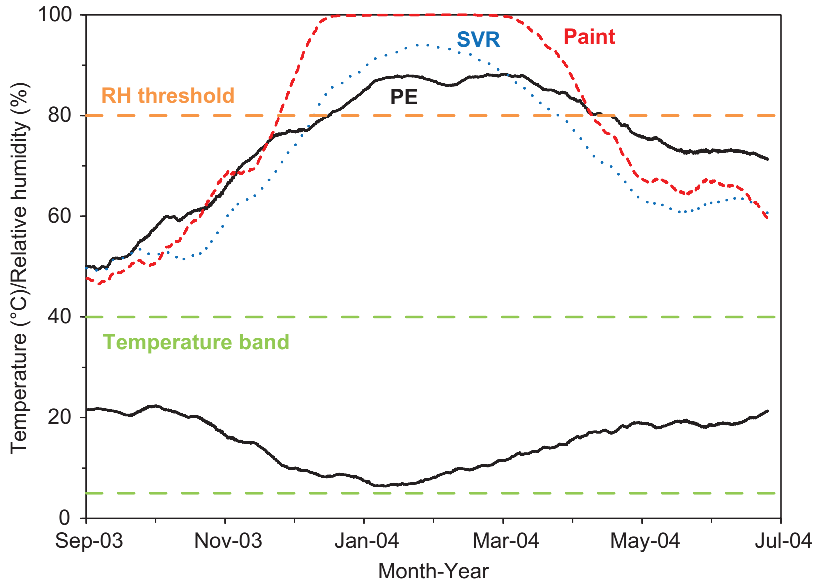

22°C and 50 % RH. Monitoring began in October 2013 and concluded when roof assemblies were inspected in June 2014. Visible mold growth was found on the cavity-side OSB surface in Roofs 4 and 5.

Hourly surface RH values are plotted in Figs. 8–10. The ventilated cathedral ceiling or compact roof assembly (Roof 1) showed large fluctuations that reflect outdoor conditions. The wafer sensor had a damped response that tracked fairly closely with the 24-h running average of the RH sensor (not shown). The OSB moisture pins also had a damped response. The other assemblies, which did not include intentional ventilation in the rafter bay, showed an expected seasonal trend of high surface RH values during winter and lower values during summer. These RH measurements are consistent with high OSB sheathing MCs measured near the ridge. In most cases for Roofs 2–7, the RH values derived from the wafer sensor and OSB moisture pins tended to lag behind the RH sensor during the autumn increase and spring decline, and they tended to read slightly higher during winter. Roofs 4 and 5 showed unusual behavior: There were significant periods in winter and spring when the RH sensors had extreme fluctuations. In Roof 4 in January, the wafer sensor dropped significantly while the OSB moisture pins dropped just

FIG. 7 Mold index values calculated from measured hourly temperature and RH values at cavity-side surface of OSB sheathing in Puyallup, WA, for walls with PE, SVR, and paint only.

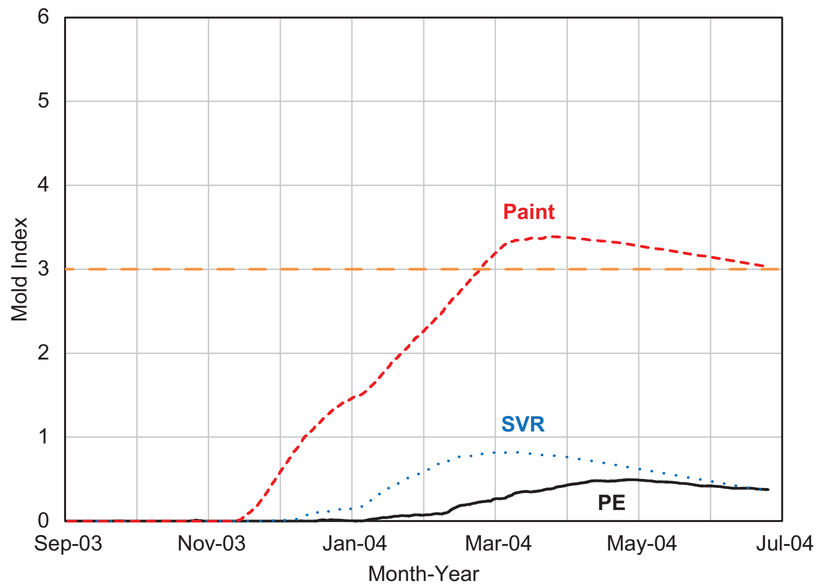

slightly. This anomalous behavior may be a result of RH sensor failure or a result of air leakage that affected the sensors in different ways. Given the visual observations of wet OSB and wet insulation, the OSB moisture pins were likely the only reliable indicator in Roof 4. In Roof 5, the wafer sensor and OSB moisture pins both remained at elevated RH from late fall to mid-spring.

The 30-day running average OSB surface RH and temperature values were analyzed previously with respect to the ASHRAE Standard 160 "Addendum a" criterion [5] by Ueno and Lstiburek [28]. The results of this analysis are summarized in Table 5. The vented compact roof was the only assembly to pass the criterion.

Mold index values calculated from the measured hourly surface RH/T values are plotted in Figs. 11–13. In Roofs 1, 2, and 6 (Fig. 11) the mold index values are well below three, the threshold for visible mold growth. In Roof 1 (vented compact roof, Fig. 11a), the mold index remains close to zero regardless of whether RH values were taken from the RH sensor or derived from the wafer sensor or OSB moisture pins. In Roof 2 (top vent cathedral, cellulose, Fig. 11b), the mold index based on all sensors stays below 2.2. In Roof 6 (diffusion vent, cellulose, Fig. 11c), the mold index calculated both ways remains below 1. These model predictions are all consistent with the lack of any visible mold growth on the cavity-side OSB surface in these assemblies.

FIG. 8 Measured hourly RH values at cavity-side surface of OSB sheathing below ridge using RH sensor, and values derived from wafer sensor and OSB moisture pins for roof assemblies 1, 2, and 6 in Bolingbrook, IL.

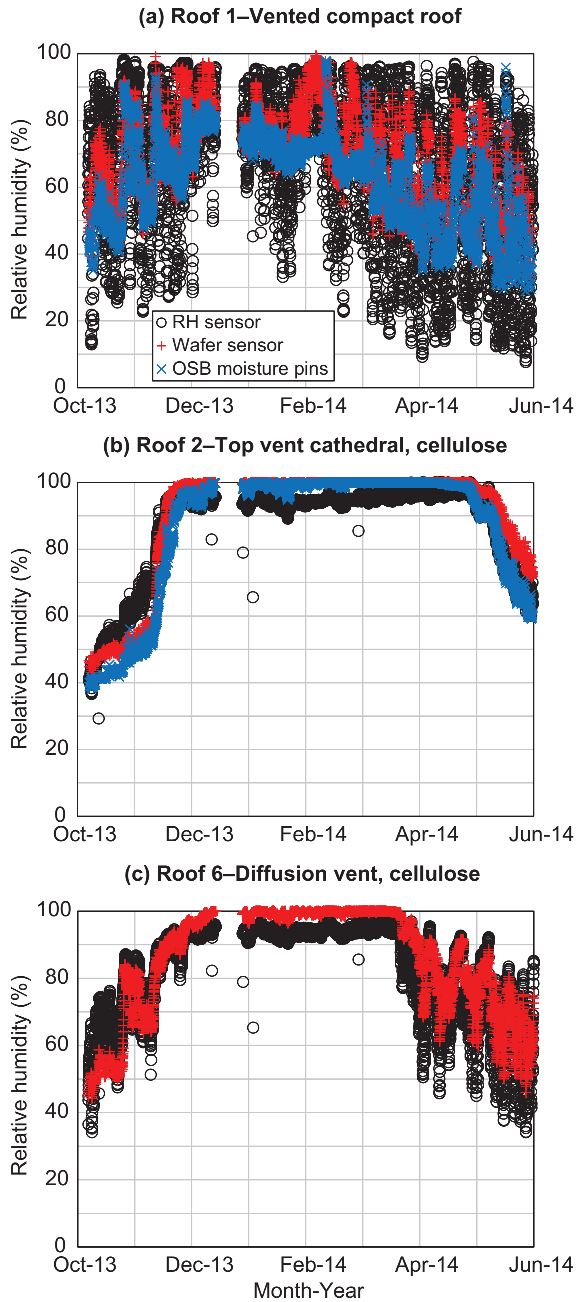

FIG. 9 Measured hourly RH values at cavity-side surface of OSB sheathing below ridge for roof assemblies 3 and 7.

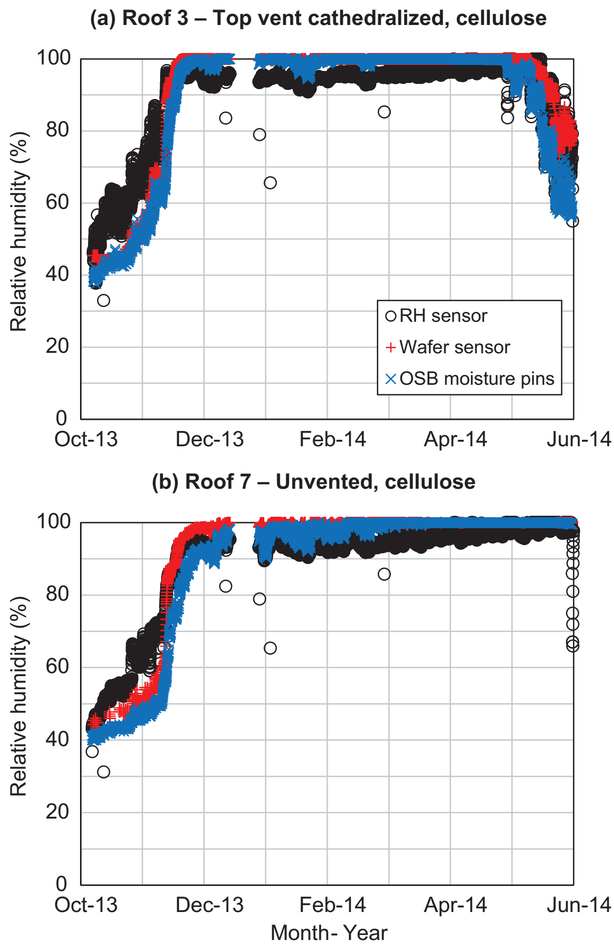

In the case of Roofs 3 and 7 (Fig. 12), the mold index values differ depending on the sensor: the wafer sensor and OSB moisture pins give higher mold index values than the RH sensor, a result of the higher RH values derived from the pin measurements (Fig. 9). In Roof 3 (top vent cathedralized, cellulose, Fig. 12a), M reaches 2.6 for the RH sensor, 3.6 for the wafer sensor, and 3.1 for the OSB moisture pins. In Roof 7 (unvented, cellulose, Fig. 12b), M reaches 2.9 for the RH sensor versus 3.5 for the wafer sensor and OSB moisture pins. No visual evidence of mold growth was observed on the cavity-side OSB surface in these assemblies; however, evidence of moisture accumulation was seen in the form of OSB grain raise, rusted staples, and cellulose insulation “caking” in Roof 7 [28]. Agreement between the mold index

FIG. 10 Measured hourly RH values at cavity-side surface of OSB sheathing below ridge for roof assemblies 4 and 5.

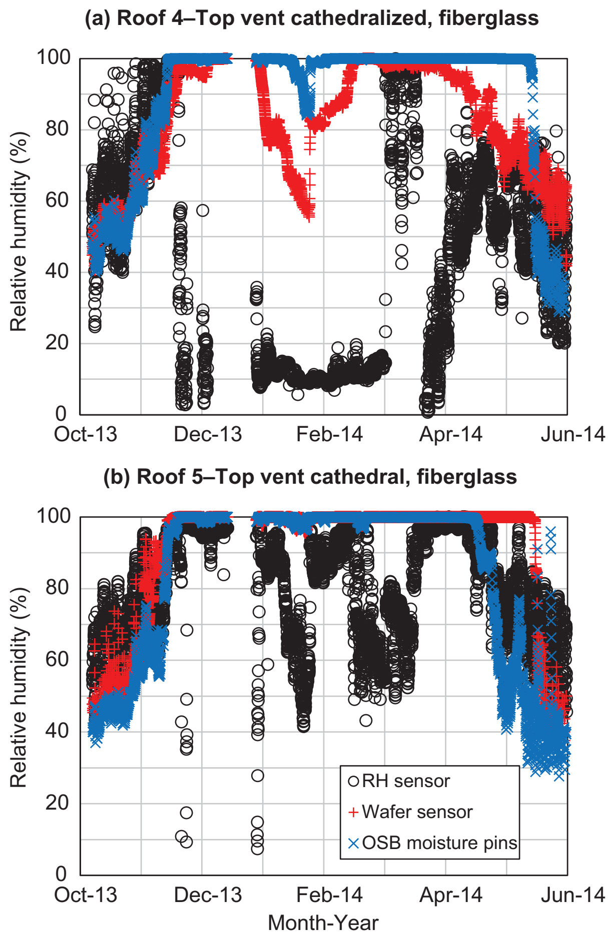

TABLE 5 Summary of analysis of roof assemblies in Bolingbrook, IL, using the 30-day criterion [28] and the mold index model (this work).

Designation	Visible Mold Growth?	Performance Model Prediction	
		30-Day Criterion	Mold Index Model
1 – Vented compact roof	No	No mold risk	M < 3
2 – Top vent cathedral, cellulose	No	Mold risk	M < 3
3 – Top vent cathedralized, cellulose	No	Mold risk	M ≈ 3 (2.6–3.6)
4 – Top vent cathedralized, fiberglass	Yes	Mold risk	Sensor-dependent
5 – Top vent cathedral, fiberglass	Yes	Mold risk	Sensor-dependent
6 – Diffusion vent, cellulose	No	Mold risk	M < 3
7 – Unvented, cellulose	No	Mold risk	M ≈ 3 (2.9–3.5)

FIG. 11 Mold index values calculated from measured hourly temperature and RH values at cavity-side surface of OSB sheathing below ridge for roof assemblies 1, 2, and 6.

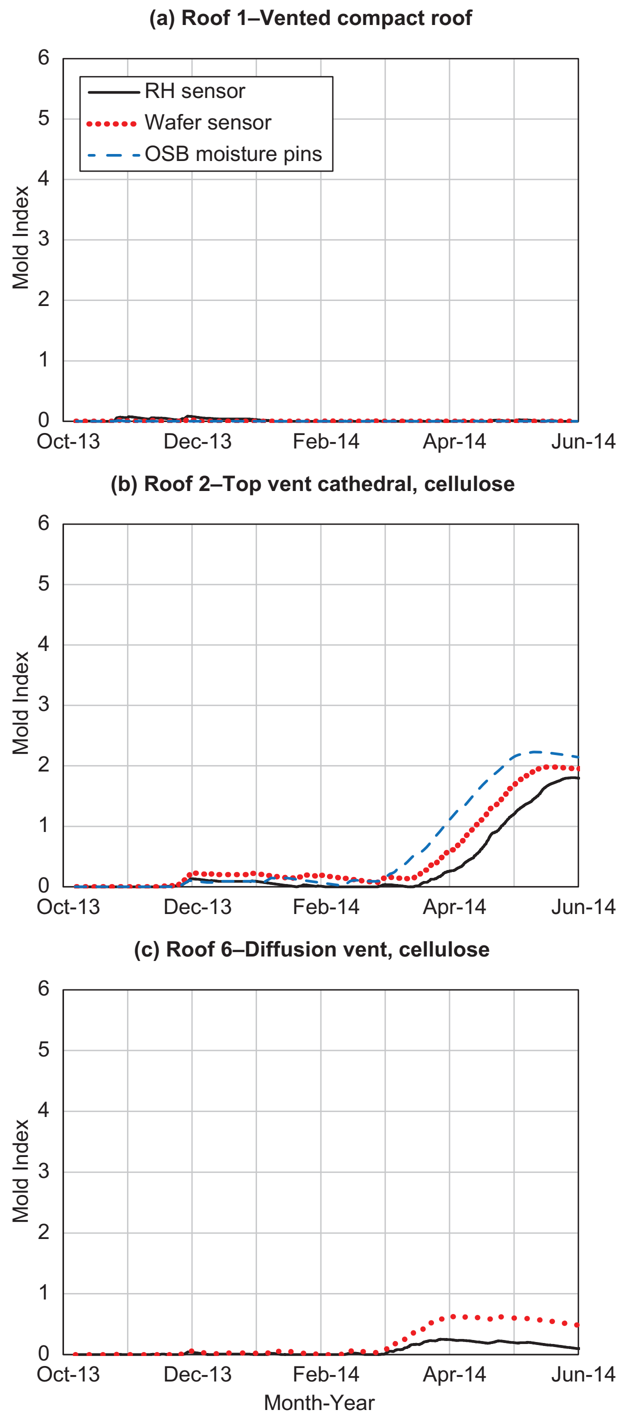

FIG. 12 Mold index values calculated from measured hourly temperature and RH values at cavity-side surface of OSB sheathing below ridge for roof assemblies 3 and 7.

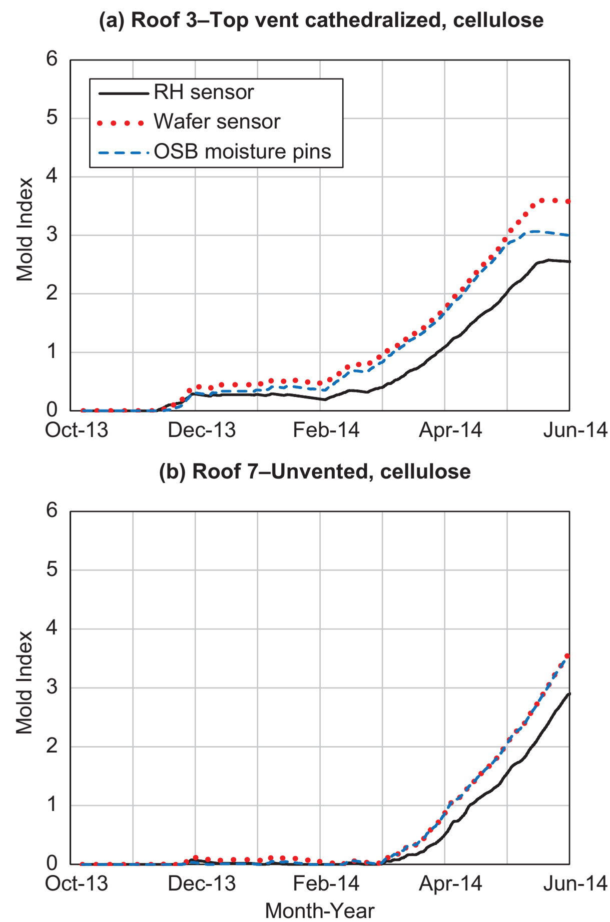

model and observation is thus considered acceptable for the RH sensor, but not for the wafer sensor or OSB moisture pins in the case of Roofs 3 and 7.

Mold index values for Roofs 4 and 5 (Fig. 13) show much larger discrepancies between the various sensors. In Roof 4 (top vent cathedralized, fiberglass, Fig. 13a), mold index peak values are less than 0.4 (RH sensor), about 2.2 (wafer sensor), and about 4.8 (OSB moisture pins). As discussed previously, the OSB moisture pins were likely the only reliable indicator in this assembly. In Roof 5 (top vent cathedral, fiberglass, Fig. 13b), peak values are M is greater than 5 for the wafer sensor, approximately 4.2 for the OSB moisture pins, and less than 2 for the RH sensor. As discussed earlier with regard to Fig. 10, the RH sensor exhibited large fluctuations,

FIG. 13 Mold index values calculated from measured hourly temperature and RH values at cavity-side surface of OSB sheathing below ridge for roof assemblies 4 and 5.

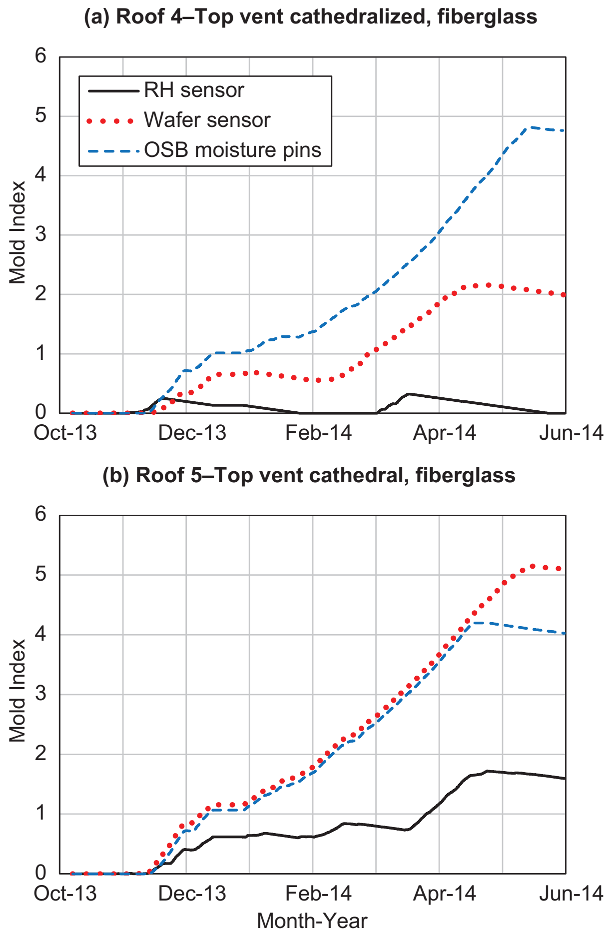

and readings may not have been reliable. The wafer sensor and OSB moisture pins were likely more reliable, though they may have overestimated the actual RH in some cases, given the pattern seen above for Roofs 3 and 7. The mold index values derived from the wafer sensor and OSB moisture pins both predicted visible mold growth but at levels higher than visually observed.

It is interesting to note that the RH values derived from the wafer sensor and OSB moisture pins in Roofs 4 and 5 (Fig. 10) are similar to those in Roofs 2, 3, and 7 (Fig. 8b and Fig. 9a and b, respectively); the mold index predictions, however, are quite different (Figs. 11–13). In Roof 5, the mold index (based on the wafer sensor and OSB moisture pins) increases gradually during the winter, whereas the other assemblies generally do not show any significant increase until spring. This wintertime increase in mold index most likely occurs because the OSB surface temperatures measured at the ridge in Roofs 4 and 5 were considerably higher in winter than in other roof assemblies (not shown), possibly high enough to support mold growth during cold winter weather. The warmer temperatures in these assemblies are further discussed by Ueno and Lstiburek [28] and may be an indication of interior-to-exterior air leakage, which would transfer heat (and moisture) to the ridge. Upon disassembly and inspection, mold growth was observed on the cavity-side surface of the OSB sheathing as well as extensive damage and staining on both sides of the OSB sheathing. The mold index values derived from OSB moisture pin measurements (Roofs 4 and 5) and wafer sensor measurements (Roof 5) predict higher coverage of mold growth than what was observed.

The analysis of the roof assemblies using both the 30-day criterion and the mold index model is summarized in Table 5. Overall, the mold index model yielded more reliable predictions than the 30-day criterion when compared to field observations. The mold index model also has the advantage of providing granularity, with a numerical scale that indicates the level of mold risk, rather than a binary pass/fail result.

Mold growth was the only evaluation criterion addressed in this analysis. Other moisture performance criteria may need to be considered in addition to mold growth, such as corrosion of fasteners [17,40] or loss of structural capacity from moisture-induced dimensional changes [17,41,42].

EXPERIMENTAL AND MODELING UNCERTAINTIES

Several sources of uncertainty both in experimental measurements and in model predictions are worthy of further discussion. The first is uncertainty in surface RH/T values derived from experimental measurements. A fundamental difficulty that has not been addressed earlier is that mold growth is related to water activity within the material at its surface. The experimental measurements are proxies for water activity. The RH/T sensor was necessarily located some distance from the material surface and measured RH in the air close to the surface. The wafer sensor, in addition to its location away from the surface, measured bulk MC of the wood wafer, which was then transformed to RH using the sorption isotherm. The OSB moisture pins measured MC at the center of the sheathing rather than the surface. In addition to the fact that the measurements are proxies, experimental error is inherent in any measurement technique. A detailed error analysis is beyond the scope of this paper, but we do present an illustration to give a sense of the impact.

The mold index for the paint wall originally presented in Fig. 7 was recalculated for two cases in which the surface RH was three percentage points higher and lower than the actual sensor measurements, to illustrate the effect of an RH sensor measurement uncertainty of ± 3 % RH. The results are shown in Fig. 14. In this example, the effect is not a simple offset. The mold index based on the measured RH – 3 % is considerably lower than the mold index based on the measured values, whereas the

FIG. 14 Effect of uncertainty in RH values on mold index. Mold index values were calculated from measured hourly temperature and RH values at cavity-side surface of OSB sheathing in Puyallup, WA, for the paint wall, the same as in Fig. 7. Mold index values were also calculated here from the measured RH ± 3 % RH (but capped at 100 % RH).

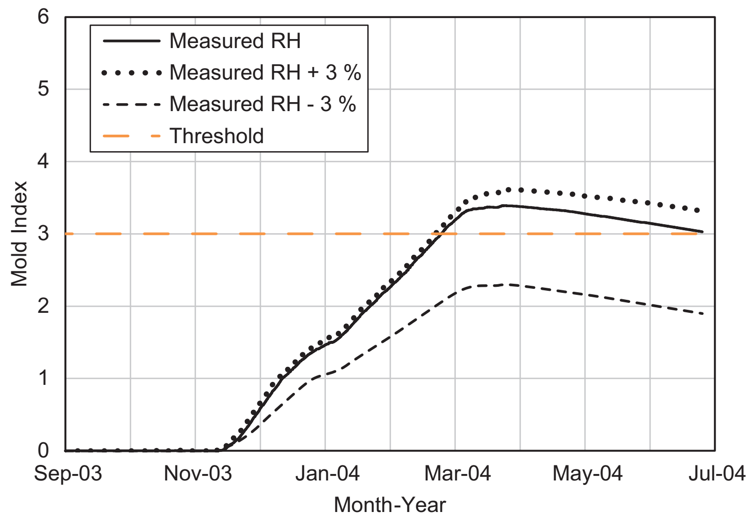

mold index based on the measured RH + 3 % (but capped at 100 % RH) is only slightly higher. A complementary illustration of the effect of RH measurement error can be seen by comparing mold index values derived from RH sensor, wafer sensor, and OSB moisture pin measurements in Fig. 11 and Fig. 12.

An additional source of uncertainty in modeling mold growth is variability in the level of mold susceptibility of the substrate material. In this analysis, we have assumed that oriented strand board can be characterized by the model parameters developed by Viitanen and colleagues for the sensitive class, which was based on materials other than OSB. It must also be recognized that OSB represents a product category, and the properties of actual OSB panels vary depending on the mix of wood species, the type and quantity of adhesive and wax, and processing temperature and pressure conditions. For instance, OSB made from southern pine was found to have higher mold susceptibility than OSB made from aspen in one study [43]. The impact of the material sensitivity class on the mold index can be seen in the illustration in Fig. 2a. Further study is recommended to better understand the variability of mold growth on wood-based sheathing products. Furthermore, the cavity insulation material adjacent to the OSB surface may have an effect on the initiation and rate of mold growth. For example, the inhibiting effects of borate additives in cellulose insulation on certain mold species have been discussed by Ueno

[33,34] and by Clausen et al. [44]. The amount of borate additive may have an effect, and it should be noted that cellulose insulation products in the United States can contain up to 20 wt% boric acid or derivatives whereas products in the European Union are limited to 5 wt%.

Finally, there is uncertainty in the initial mold index value at the beginning of the field monitoring studies. The analysis presented here has assumed that the mold index was zero when monitoring began. This assumption is necessary because the prior history of the OSB panels was not documented. The prior history, however, could possibly have involved some wetting during outdoor storage on the job site or during construction. Such wetting could have led to microscopic levels of mold growth.

Conclusions

This paper provides an overview of the evaluation criteria for mold growth in ASHRAE Standard 160, *Criteria for Moisture-Control Design Analysis in Buildings*, and an overview of the mold growth model developed by Viitanen and colleagues. The objective of the analysis described here was to compare the predictive ability of the simple 30-day running average criterion in ASHRAE Standard 160 to the mold index model. The two methods used hourly measured surface RH and temperature values as inputs, and results were compared with field observations of mold growth (or lack thereof) in various building envelope assemblies.

Prior analysis by the authors (Table 4) indicated that, in all but one case, the 30-day criterion failed assemblies in which visible mold growth was not observed during disassembly; that is, the hourly measured surface RH/T conditions led to calculated 30-day running averages that did not stay within the specified "conditions necessary to minimize mold growth." In all cases, the mold index model, using measured hourly surface RH/T values as inputs, resulted in mold index values less than three. This is the threshold for visual finding of mold growth (without magnification), so the mold index model predictions were in agreement with observations.

Three wall assemblies monitored near Seattle, WA, were analyzed here using the 30-day criterion and the mold index model. Visible mold growth was observed during inspection on the cavity-side surface of OSB sheathing in the wall with paint as the only vapor retarder. The 30-day criterion failed all three assemblies. The mold index model yielded a value above three for the paint wall, in agreement with visual observation, and mold index values well below three for the wall with PE and polyamide vapor retarders, which agreed with the lack of any visible mold.

The analysis also considered seven roof assemblies that were monitored in a test house near Chicago, IL. Visible mold growth was found on the cavity-side surface of OSB roof sheathing in two of these seven test bays, both of which had anomalous RH sensor readings. Out of the five remaining assemblies, the 30-day criterion failed all but one. The mold index model was run with RH values derived from an RH sensor, a wafer sensor, and moisture pins in the OSB sheathing. Three of the assemblies without visible mold growth had mold index values well below three. Two assemblies, also without visible mold growth but with indication of significant moisture accumulation, had mold index values slightly below three using the RH sensor and slightly above three using the wafer sensor and OSB moisture pins. The assemblies with visible mold growth had questionable RH sensor readings, and the mold index values derived from wafer sensor measurements were inconsistent. Visible mold growth was not predicted in one assembly but was predicted at higher coverage than observed in the other assembly. For both assemblies, visible mold growth at higher coverage than observed was predicted from the OSB moisture pins.

Overall, the mold index model yielded more reliable predictions than the 30-day criterion when compared to field observations. The mold index model also has the advantage of providing granularity, with a numerical scale that indicates the level of mold risk, rather than a binary pass/fail result. The sources of uncertainty in experimental measurements and the impact on the calculated mold index were illustrated. Additional sources of uncertainty in modeling mold growth include the degree to which model parameters for a particular sensitivity class capture the behavior of the actual material, potential inhibiting effects of borate treatment in cellulose insulation, and lack of information on the initial mold index at the start of an analysis. Despite these uncertainties, the mold index model is a significant improvement over the 30-day criterion in ASHRAE Standard 160.

ACKNOWLEDGMENT

The authors thank Chuck Murray of the Washington State Department of Commerce, Energy Policy Division, for exhuming and sharing data from the Natural Exposure Test Facility in Puyallup, WA. Samuel V. Glass acknowledges support of the U.S. Department of Agriculture, Forest Service, Forest Products Laboratory.

References

[1] ANSI/ASHRAE Standard 160-2009, *Criteria for Moisture-Control Design Analysis in Buildings*, American Society of Heating, Refrigerating and Air-Conditioning Engineers, Atlanta, GA, 2009, www.ashrae.org

[2] TenWolde, A., "A Review of ASHRAE Standard 160—Criteria for Moisture Control Design Analysis in Buildings," *J. Test. Eval.*, Vol. 39, No. 1, 2011, pp. 77–81, http://dx.doi.org/10.1520/JTE102896

[3] Gatland II, S. D., "Predicting the Hygrothermal Performance of Commercial Building Envelope Systems Using Computer Modeling Techniques Outlined in ASHRAE Standard 160-2009," *Proceedings of the RCI 25th International Convention*, Orlando, FL, March 24–30, 2010, Roof Consultants Institute.

[4] International Energy Agency, "Report Annex XIV: Condensation and Energy, Vol. 1: Sourcebook," Leuven, Belgium, 1991.

[5] ANSI/ASHRAE, "Addendum a to ANSI/ASHRAE Standard 160-2009," American Society of Heating, Refrigerating and Air-Conditioning Engineers, Atlanta, GA, 2011, www.ashrae.org

[6] Drumheller, S. C. and Carll, C. G., "Effect of Cladding Systems on Moisture Performance of Wood-Framed Walls in a Mixed-Humid Climate," *Thermal Performance of the Exterior Envelopes of Whole Buildings XI International Conference*, Clearwater Beach, FL, December 5–9, 2010, American Society of Heating, Refrigerating and Air-Conditioning Engineers, Atlanta, GA.

[7] Arena, L. B. and Mantha, P., "Moisture Research—Optimization of Wall Assemblies," U.S. Department of Energy Building America Technical Report, Consortium for Advanced Residential Buildings, Norwalk, CT, 2012.

[8] Ueno, K. and Lstiburek, J., "Guidance on Modeling Enclosure Design in Above Grade Walls: Expert Meeting Report," *Building America Report 1403*, Building Science Corporation, Westford, MA, 2014.

[9] Glass, S. V., Schumacher, C., and Ueno, K., "The Long and Winding Road: Remediation of ASHRAE 160," *Westford Symposium on Building Science XIX*, Westford, MA, August 3–5, 2015, https://buildingscience.com/sites/default/files/03.02_2015-08-05_ashrae_160_glass_schumacher_ueno.pdf (accessed November 14, 2016).

[10] Lstiburek, J., Ueno, K., and Musunuru, S., "Modeling Enclosure Design in Above Grade Walls," *Building America Report 1509*, Building Science Corporation, Westford, MA, 2015.

[11] Viitanen, H. and Ritschkoff, A.-C., "Mould Growth in Pine and Spruce Sapwood in Relation to Air Humidity and Temperature," *Report No 221*, Swedish University of Agricultural Sciences, Department of Forest Products, Uppsala, Sweden, 1991.

[12] Viitanen, H., "Factors Affecting the Development of Mould and Brown Rot Decay in Wooden Material and Wooden Structures: Effect of Humidity, Temperature and Exposure Time," Ph.D. dissertation, Swedish University of Agricultural Sciences, Department of Forest Products, Uppsala, Sweden, 1996.

[13] Hukka, A. and Viitanen, H. A., "A Mathematical Model of Mould Growth on Wooden Material," *Wood Sci. Technol.*, Vol. 33, No. 6, 1999, pp. 475–485.

[14] Clarke, J. A., Johnstone, C. M., Kelly, N. J., McLean, R. C., Anderson, J. A., Rowan, N. J., and Smith, J. E., "A Technique for the Prediction of the Conditions Leading to Mould Growth in Buildings," *Build. Environ.*, Vol. 34, No. 4, 1999, pp. 515–521, http://dx.doi.org/10.1016/S0360-1323(98)00023-7

[15] Hens, H. L. S. C., "Fungal Defacement in Buildings: A Performance Related Approach," *HVAC&R Res.*, Vol. 5, No. 3, 1999, pp. 265–280.

[16] Sedlbauer, K., "Prediction of Mould Fungus Formation on the Surface of and Inside Building Components," Ph.D. dissertation, University of Stuttgart, 2001.

[17] Viitanen, H., and Salonvaara, M., "Failure Criteria," *Moisture Analysis and Condensation Control in Building Envelopes, ASTM MNL40*, H. R. Trechsel, Ed., ASTM International, West Conshohocken, PA, 2001, pp. 66–80, www.astm.org

[18] Vereecken, E. and Roels, S., "Review of Mould Prediction Models and Their Influence on Mould Risk Evaluation," *Build. Environ.*, Vol. 51, 2012, pp. 296–310, http://dx.doi.org/10.1016/j.buildenv.2011.11.003

[19] Vereecken, E., Vanoirbeek, K., and Roels, S., "Towards a More Thoughtful Use of Mould Prediction Models: A Critical View on Experimental Mould Growth Research," *J. Build. Phys.*, Vol. 39, No. 2, 2015, pp. 102–123, http://dx.doi.org/10.1177/1744259115588718

[20] BSR/ASHRAE, "Addendum e to ANSI/ASHRAE Standard 160-2009," *Criteria for Moisture-Control Design Analysis in Buildings*, First Public Review Draft, American Society of Heating, Refrigerating and Air-Conditioning Engineers, Atlanta, GA, 2016.

[21] Ojanen, T., Viitanen, H., Peuhkuri, R., Lähdesmäki, K., Vinha, J., and Salminen, K., "Mold Growth Modeling of Building Structures Using Sensitivity Classes of Materials," *Thermal Performance of the Exterior Envelopes of Buildings XI International Conference*, Clearwater Beach, FL, December 5–9, 2010, American Society of Heating, Refrigerating and Air-Conditioning Engineers, Atlanta, GA.

[22] Viitanen, H., "Factors Affecting the Development of Biodeterioration in Wooden Constructions," *Mater. Struct.*, Vol. 27, No. 8, 1994, pp. 483–493.

[23] Viitanen, H. and Bjurman, J., "Mold Growth on Wood under Fluctuating Humidity Conditions," *Mater. Organismen*, Vol. 29, 1995, pp. 27–46.

[24] Viitanen, H. A., "Modelling the Time Factor in the Development of Mould Fungi—The Effect of Critical Humidity and Temperature Conditions on Pine and Spruce Sapwood," *Holzforschung*, Vol. 51, No. 1, 1997, pp. 6–14, http://dx.doi.org/10.1515/hfsg.1997.51.1.6

[25] Viitanen, H. and Ojanen, T., "Improved Model to Predict Mold Growth in Building Materials," *Thermal Performance of the Exterior Envelopes of Whole Buildings X International Conference*, Clearwater Beach, FL, December 2–7, 2007, American Society of Heating, Refrigerating and Air-Conditioning Engineers, Atlanta, GA.

[26] Viitanen, H., Vinha, J., Salminen, K., Ojanen, T., Peuhkuri, R., Paajanen, L., and Lähdesmäki, K., "Moisture and Bio-deterioration Risk of Building Materials and Structures," *J. Build. Phys.*, Vol. 33, No. 3, 2010, pp. 201–224, http://dx.doi.org/10.1177/1744259109343511

[27] Gatland II, S. D., Karagiozis, A. N., Murray, C., and Ueno, K., "The Hygrothermal Performance of Wood-Framed Wall Systems Using a Relative Humidity-Dependent Vapor Retarder in the Pacific Northwest," *Thermal Performance of the Exterior Envelopes of Whole Buildings X International Conference*, Clearwater Beach, FL, December 2–7, 2007, American Society of Heating, Refrigerating and Air-Conditioning Engineers, Atlanta, GA.

[28] Ueno, K. and Lstiburek, J. W., "Field Testing Unvented Roofs with Asphalt Shingles in Cold and Hot-Humid Climates," *Building America Report 1409*, Building Science Corporation, Westford, MA, 2015.

[29] Carll, C. and TenWolde, A., "Accuracy of Wood Resistance Sensors for Measurement of Humidity," *J. Test. Eval.*, Vol. 24, No. 3, 1996, pp. 154–160, https://dx.doi.org/10.1520/JTE11296J

[30] Ueno, K. and Straube, J., "Laboratory Calibration and Field Results of Wood Resistance Humidity Sensors," *Building Enclosure Science & Technology (BEST1): Building for Energy Efficiency and Durability at the Crossroads: Bugs Mold and Rot IV*, Minneapolis, MN, June 10–12, 2008.

[31] Straube, J., Onysko, D., and Schumacher, C., "Methodology and Design of Field Experiments for Monitoring the Hygrothermal Performance of Wood Frame Enclosures," *J. Therm. Envelope Build. Sci.*, Vol. 26, No. 2, 2002, pp. 123–151, http://dx.doi.org/10.1177/0075424202026002098

[32] Glass, S. V., and Zelinka, S. L., "Moisture Relations and Physical Properties of Wood," *Wood Handbook—Wood as an Engineering Material*, General Technical Report FPL–GTR–190, R. J. Ross, Ed., U.S. Department of Agriculture, Forest Service, Forest Products Laboratory, Madison, WI, 2010, pp. 4.1–4.19.

[33] Ueno, K., "Monitoring of Double-Stud Wall Moisture Conditions in the Northeast," *Building America Report 1501*, Building Science Corporation, Westford, MA, 2015.

[34] Ueno, K. and Lstiburek, J., "Field Monitoring for Cold-Climate Double Stud Walls with Cellulose and Low Density Foam Insulation," *Building Enclosure Science & Technology (BEST4): Performance Driven Architectural Design*, Kansas City, MO, April 12–15, 2015.

[35] Schumacher, C. J. and Reeves, E., "Field Performance of an Unvented Cathedral Ceiling (UCC) in Vancouver," *Thermal Performance of the Exterior Envelopes of Whole Buildings X International Conference*, Clearwater Beach, FL, December 2–7, 2007, American Society of Heating, Refrigerating and Air-Conditioning Engineers, Atlanta, GA.

[36] Schumacher, C. J., "Hygrothermal Performance of Insulated, Sloped, Wood-Framed Roof Assemblies," Master's thesis, University of Waterloo, Department of Civil Engineering, Waterloo, ON, 2008.

[37] ASHRAE, "Heat, Air, and Moisture Control in Building Assemblies—Material Properties," *2013 ASHRAE Handbook: Fundamentals*, American Society of Heating, Refrigerating and Air-Conditioning Engineers, Atlanta, GA, 2013, p. 26.16.

[38] Gatland II, S. D., "Comparison of Water Vapor Permeance Data of Common Interior Building Materials in North American Wall Systems," *Proceedings of the 10th Canadian Conference on Building Science and Technology*, Ottawa, ON, May 12–13, 2005, pp. 182–194.

[39] Tichy, R. and Murray, C., "Developing Innovative Wall Systems that Improve Hygrothermal Performance of Residential Buildings," *Final Report to U.S. Department of Energy*, Washington State University, Pullman, WA, 2007.

[40] Zelinka, S., "Corrosion of Metals in Wood Products," *Developments in Corrosion Protection*, M. Aliofkhazraei, Ed., *InTech*, 2014, pp. 567–592, http://dx.doi.org/10.5772/57296

[41] Home Innovation Research Labs, "Characterization of the Moisture Performance of Energy-Efficient and Conventional Light-Frame Wood Wall Systems," Home Innovation Research Labs, Upper Marlboro, MD, 2013.

[42] Carll, C. and Wiedenhoeft, A. C., "Moisture-Related Properties of Wood and the Effects of Moisture on Wood and Wood Products," *Moisture Control in Buildings: The Key Factor in Mold Prevention*, H. R. Trechsel and M. T. Bomberg, Eds., 2nd ed, ASTM International, West Conshohocken, PA, 2009, pp. 54–79.

[43] Ye, X., Wang, S., Ruan, R., Qi, J., Womac, A. R., and Doona, C. J., "Water Mobility and Mold Susceptibility of Engineered Wood Products," *Trans. ASABE*, Vol. 49, No. 4, 2006, pp. 1159–1165.

[44] Clausen, C. A., Glaeser, J. A., Glass, S. V., and Carll, C., "Occurrence of Mold in a Two-Story Wood-Frame House Operated at Design Indoor Humidity Levels," *General Technical Report FPL–GTR–186*, U.S. Department of Agriculture, Forest Service, Forest Products Laboratory, Madison, WI, 2009.